Molecular Biotechnology (2024) 66:626–640
https://doi.org/10.1007/s12033-022-00595-w

ORIGINAL PAPER

Proteome-Based Investigation Identified Potential Drug Repurposable Small Molecules Against Monkeypox Disease

Arittra Bhattacharjee[1] · Ishtiaque Ahammad[1] · Zeshan Mahmud Chowdhury[1] · Keshob Chandra Das[2] · Chaman Ara Keya[3] · Md. Salimullah[2]

Received: 16 August 2022 / Accepted: 25 October 2022 / Published online: 10 November 2022

Abstract

Monkeypox Virus (MPXV), the causative agent of Monkeypox (MPX) disease, is an emerging zoonotic pathogen spreading in different endemic and non-endemic nations and creating outbreaks. MPX treatment mainly includes Cidofovir and Tecovirimat but they have several side effects and solely depending on these drugs may promote the emergence of drug-resistant variants. Hence, new drugs are required to control the spread of the disease. In this study, we explored the MPXV proteome to suggest repurposable drugs. DrugBank screening revealed drugs such as Brinzolamide, Dorzolamide, Methazolamide, Zidovudine, Gemcitabine, Hydroxyurea, Fludarabine, and Tecovirimat as controls. Structural analogs of these compounds were extracted from ChEMBL Database. After Molecular docking and Absorption, Distribution, Metabolism, Excretion, and Toxicity (ADMET)-based screening, we identified Zidovudine (binding affinity-5.9 kcal/mol) and a Harmala alkaloid (2S,4R)-4-(9H-Pyrido[3,4-b]indol-1-yl)-1,2,4-butanetriol (binding affinity − 6.6 kcal/mol) against L2R receptor (Thymidine Kinase). Moreover, Fludarabine (binding affinity − 6.4 kcal/mol) and 5′-Dehydroadenosine (binding affinity − 6.4 kcal/mol) can strongly interact with the I4L receptor (Ribonucleotide reductase large subunit R1). Molecular Dynamics (MD) simulations suggest all of these compounds can change the C-alpha backbone, residue mobility, compactness, and solvent accessible surface area of L2R and I4L. Our results strongly suggest that these drug repurposing small molecules are worth exploring in vivo and in vitro for clinical applications.

Keywords Monkeypox · Zidovudine · Fludarabine · L2R · I4L · MD simulation

Introduction

Monkeypox Virus (MPXV), an enveloped double-stranded DNA virus, belongs to the *Orthopoxvirus* genus and *Poxviridae* family. MXPV is the causative agent of the emerging zoonotic disease Monkeypox (MPX) [1]. Since May 2022, cases of MPXV infection have been reported in non-endemic nations, such as the USA, the UK, Germany, and Australia (https://www.who.int/emergencies/disease-outbreak-news/item/2022-DON385). These cases are alarming and indicate an emerging epidemic. MPXV has the ability to infect large mammalian species. This virus can be spread through saliva or respiratory substances, as well as skin contact with lesion exudate or crust material. MPXV can be shredded from the feces of infected people [2, 3]. From the contaminated sources, *Orthopoxvirus* such as MPXV generally interacts with host glycosaminoglycans (GAGs) and enters into the host cell via endocytosis [4]. In the early phase of infection, the viral DNA gets transcribed in the host cytoplasm via viral RNA polymerase. In the Intermediate phase, the uncoated virus proceeds to replicate the double-stranded DNA. After the synthesis of structural proteins in the late phase, it constructs an intracellular mature virion (IMV). The IMV virion can be released by cell lysis or it can acquire a layer of the double membrane by trans-Golgi and come out as an external enveloped virion (EEV) (https://viralzone.expasy.org/149). The immune system responds when it

✉ Md. Salimullah
salim2969@gmail.com

[1] Bioinformatics Division, National Institute of Biotechnology, Ganakbari, Ashulia, Savar, Dhaka 1349, Bangladesh

[2] Molecular Biotechnology Division, National Institute of Biotechnology, Ganakbari, Ashulia, Savar, Dhaka 1349, Bangladesh

[3] Department of Biochemistry and Microbiology, North South University, Bashundhara, Dhaka 1229, Bangladesh

faces the viral DNA. This is critical for both defense and the establishment of adaptive unity. Usually cyclic GMP–AMP synthase (cGAS), IFN-γ-inducible protein 16 (IFI16), and DNA-dependent protein kinase (DNA-PK) sense viral DNA and initiate an innate response [5]. The clinical symptoms of MPX and Smallpox infection are not very distinguishable. Except for lymph node enlargement, which occurs early, often at the onset of fever, the majority of clinical characteristics of human MPX infection are similar to those of Smallpox [6].

Cidofovir, chemical name [(2S)-1-(4-amino-2-oxopyrimidin-1-yl)-3-hydroxypropan-2-yl] oxymethylphosphonic acid, is commonly used to treat MPX patients. Sometimes Brincidofovir (prodrug of Cidofovir) is also given. Cidofovir is an antiviral medicine that works against a variety of DNA viruses, including smallpox, MPX, cowpox, variola, and vaccinia. This medication can be given intravenously or topically [7]. Cidofovir is phosphorylated intracellularly after administrations and transforms into a cytosine analog. Because this cytosine analog competes with cytosine, viral DNA chain synthesis is stopped. Although the efficacy of the drug is satisfactory, this compound can lead to hepatotoxicity or nephrotoxicity in some patients [8]. Another antiviral drug called Tecovirimat is effective against MPX. This compound inhibits the functional role of the viral envelope protein. This inhibition leads to a reduced amount of extracellular virus; hence, the viral spreading decreases after treatment [9]. However, the drug is under investigation. It might take a long time to get established for the usage of this drug for MPX treatment.

MPX infections can be handled more efficiently using safer drugs. Drug repurposing and rational exploration of new drugs using bioinformatics tools are a fast and prospective approach to achieving this goal [10, 11]. In this study, we searched the proteome of MPXV to identify new drugs that are approved or very similar to the approved drugs. We conducted virtual screening and measured the Absorption, Distribution, Metabolism, and Toxicity (ADMET) values of the selected drugs. Using molecular docking and molecular dynamics (MD) simulations, we finally predicted some plausible anti-MPXV drugs.

Method

Drug Compound Selection

The total reference proteome of Monkeypox virus Zaire-96-I-16 (NCBI Accession ID: NC_003310.1) was collected from the National Center for Biotechnology Information (NCBI) Virus database. All proteins went under Basic Local Alignment Tool (BLAST)-based searching using DrugBank BlastP (https://go.drugbank.com/structures/search/bonds/sequence) for detecting druggable candidates. Drug targets and drugs with bit score higher than 100 and E value less than 0.001 were taken as a potential drugs and drug targets [12]. Only approved drugs (except Tecovirimat which is currently administered as an antiviral against MPX) were taken for further explorations.

Similar Drug Search

Drugs with similar structures were detected using Swiss-Similarity (http://www.swisssimilarity.ch/). Here, the SMILES of the selected approved drugs were given. Using the Bioactive Class of Compounds, Three-Dimensional (3D) parameters, and the ChEMBL database (https://www.ebi.ac.uk/chembl/), similar structures were detected. Compound library and screening method was Electroshape. Compounds with ≥ 0.9 score were considered very similar structures [13]. The SMILES were converted into pdb via Online SMILES Translator and Structure File Generator (https://cactus.nci.nih.gov/translate/).

Receptor Preparation

Proteins that were potential targets for the approved compounds went under homology modeling. The primary sequences of the proteins were taken from the NCBI protein database. The primary sequences were given in AlphaFold2. This software was implemented via Colabfold [14, 15]. The models were refined by GalaxyRefine [16]. The receptors were visualized by University of California San Francisco (UCSF) ChimeraX [17]. The refined models were evaluated by SAVES v6.0 (https://saves.mbi.ucla.edu/) using ERRAT, Verify3D, and PROCHECK [18–20].

Molecular Docking

The selected receptors and ligands were imported in PyRx (https://pyrx.sourceforge.io/). PyRx is an open source tool that uses OpenBabel, AutoDock 4, and AutoDock Vina [21–24]. The ligands and receptors were converted into pdbqt format via OpenBabel. To draw the box for docking, the maximize option was selected. The maximize option covered the entire receptor. The molecular docking was performed to identify binding affinity of the selected molecules. To identify the inhibition constant (Ki) of the selected compounds, formula $Ki = \exp(\Delta G/RT)$ is implemented. Here, ΔG is the binding affinity or binding energy, R is the universal gas constant ($1.985 \times 10 - 3$ kcal/mol/K), and the value of temperature T was 25 °C (298.15 K) (Ortiz et al. 25).

ADMET Screening

Approved drugs were taken as control. Analogs of these control drugs went under molecular docking. Analogs that showed more binding affinity scores than their corresponding control drugs were selected for Absorption, Distribution, Metabolism, Excretion, and Toxicity (ADMET) analysis. To do so, the Canonical Simplified Molecular Input Line Entry System (SMILES) that were generated by SwissSimilarity were given in pkCSM (http://biosig.unimelb.edu.au/pkcsm/). Analogs with AMES test negative, hepatotoxicity negative, and highest intestinal absorption were visualized.

Ligand–Receptor Visualization

The pdbqt output of the selected ligands and receptors are imported in PyMol [26]. The ligand–receptor complexes were generated in PyMol. Finally, the molecular visualization was conducted via BIOVIA Discovery Studio Visualizer (https://discover.3ds.com/).

Molecular Dynamics Simulations

The ligand–receptor complexes were uploaded in Chemistry at Harvard Macromolecular Mechanics-Graphical User Interface (CHARMM-GUI)(https://www.charmm-gui.org/) input generator using the solution builder option [27]. Inputs were generated for GROningen MAchine for Chemical Simulations (GROMACS) 2021[28]. A transferable intermolecular potential with 3 points (TIP3) water box was created with 1-nm distance. CHARMM36m force field was implemented for energy minimization along with 100-ps NVT and NPT simulations at 303.15-K temperature [29]. Afterward, 100-ns production simulation was conducted. To analyze the secondary structure contents during simulation, gmx do_dssp of GROMACS was implemented.

Results

The workflow of the total study is presented in Fig. 1.

E8L and I4L Showed Three of Potential Approved Drugs Against Them

Monkeypox virus complete genome (NCBI Reference Sequence: NC_003310.1) had 181 proteins. All of these proteins went through Drug Bank BlastP. Among them, E8L or IMV surface membrane protein (32 kDa) that binds to cell surface chondroitin sulfate (glycosaminoglycan) and I4L or ribonucleotide reductase large subunit R1 showed highest (3) matches with approved drugs. E8L showed Brinzolamide, Dorzolamide, and Methazolamide. I4L matched with Gemcitabine, Hydroxyurea, and Fludarabine. Other proteins, such as L2R and Phospholipase-D-like protein, matched with Zidovudine and Tecovirimat, respectively (Table 1).

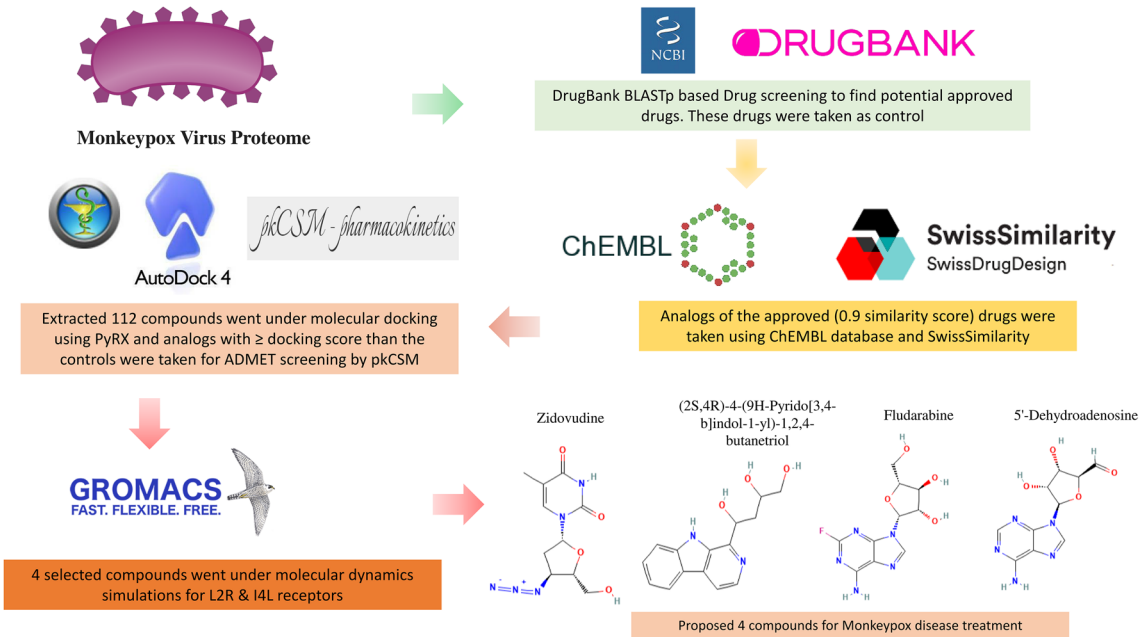

Fig. 1 Schematic representation of the total study

Table 1 Drug Bank BlastP results of approved drugs against the monkeypox virus proteome

Protein (NCBI_accession)	*E*-value	Bit score	Drug name	Drug group
E8L (NP_536532.1)	2.53E-42	145.591	Brinzolamide, Dorzolamide, Methazolamide	Approved
L2R (NP_536513.1)	8.99E-87	253.447	Zidovudine	Approved
I4L (NP_536492.1)	0	1161.75	Gemcitabine, Hydroxyurea, Fludarabine	Approved
Phospholipase-D-like protein (NP_536457)	6.05E-28	112.464	Tecovirimat	Approved & investigational

Antineoplastic Fludarabine and Antiretroviral Zidovudine Had Highest Amount of Analogs

SwissSimilarity detected compounds with different scores with the Electroshape method. The Electroshape method calculated fast molecular similarity calculations with chirality, shape and electrostatics in the ChEMBL database (https://www.ebi.ac.uk/chembl/) [30]. Here, most of the approved drugs did not have enormous analogs with 90% similarity. Only Fludarabine and Zidovudine presented 70 and 28 analogs, respectively (Table 2). Total 112 compounds were taken for molecular docking (Fig. 2).

Molecular Docking Followed by ADMET Screening Predicted Potential Fludarabine and Zidovudine Analogs

The approved drugs and the model validations were conducted. All of the proteins showed > 90% of their amino acids in most favored regions. Analogs were docked against their corresponding receptors. To do so, 3D models of the viral proteins were generated and refined. All of them had an ERRAT score more than 90. Except for E8L, all of them passed the Verify3D test (Fig. 3).

Fifteen Zidovudine analogs scored better than Zidovudine. One analog showed an equal score. Twenty-Five Fludarabine analogs performed better than the parent drug. Eight compounds showed the same scores. Tecovirimat demonstrated one better compound with higher binding affinity. E8L had four ligands with more binding affinity than approved drugs.

Except CHEBI 43411, CHEBI 6822, and Methazolamide, all of the compounds demonstrated Ki value less than 100 µM.

The outperformed ligands and the approved drugs of Table 3 went under ADMET screening. The SMILES were given in pkCSM. pkCSM predicted the ADMET properties via graph-based signatures. Ligands with Hepatotoxic and mutagenic (AMES-positive) properties were discarded.

(2S,4R)-4-(9H-Pyrido[3,4-b]indol-1-yl)-1,2,4-butanetriol or CHEBI: 173933 had highest intestinal absorption (92.641%). 5'-Dehydroadenosine or CHEBI: 1958 showed 51.647% intestinal absorption. CHEBI: 173933 had highest Caco2 permeability 1.085. The unbound fraction (Fu) values were 0.755, 0.137, 0.86, and 0.81 for Zidovudine, CHEBI: 173933, Fludarabine, CHEBI: 1958, respectively. All of these molecules cannot cross the blood–brain barrier or Central Nervous System (CNS). Only CHEBI: 173933 might act as a CYP1A2 inhibitor. Total Clearance (log ml/min/kg) were 0.052, 0.663, 0.703 and 0.793 for Zidovudine, (2S,4R)-4-(9H-Pyrido[3,4-b]indol-1-yl)-1,2,4-butanetriol, Fludarabine, and 5′-Dehydroadenosine, respectively. Only Fludarabine was AMES-positive and other drugs were AMES negative. Both approved drugs Zidovudine and Fludarabine had been classified as hepatotoxic by pkCSM. However, 5′-Dehydroadenosine and (2S,4R)-4-(9H-Pyrido[3,4-b]indol-1-yl)-1,2,4-butanetriol had no hepatotoxic properties.

Ligand–receptor visualization demonstrated that (2S,4R)-4-(9H-Pyrido[3,4-b]indol-1-yl)-1,2,4-butanetriol (CHEBI: 173933) engaged more residues and generated less unflavored bonds with L2R (Thymidine Kinase) than Zidovudine. Especially, the Harmala alkaloid part of this compound generated Pi-sigma and Amide-Pi-stacked bond with the Thymidine kinase and allowed more solvent-accessible area (Sky blue shades in the benzene ring of Fig. 4b). This was not observed for Zidovudine (Fig. 4) (https://hmdb.ca/metabolites/HMDB0035191).

MD Simulations Based Insights Were Very Similar for All Druggable Candidates

Molecular dynamics simulation was carried out for the selected ligand–receptor complexes. The simulations generated Root Mean Square Deviation (RMSD), Root Mean Square Fluctuations (RMSF), Radius of Gyration (Rg), and Solvent-Accessible Surface Area (SASA) (Fig. 5).

RMSD of L2R (Thymidine Kinase) C-alpha backbone with Zidovudine (Green) and (2S,4R)-4-(9H-Pyrido[3,4-b] indol-1-yl)- 1,2,4-butanetriol (CHEBI: 173933) (Golden) showed around similar value of RM hiSD from 0 to 50 ns. After 50 ns, around 0.1 ns or 1 Å (Fig. 6a). The RMSF values or protein mobility were very similar for both of the compounds (Fig. 6b). The values of protein compactness (Rg) increased by the time and with more SASA (Fig. 6c and d).

I4L (Ribonucleotide reductase large subunit R1) with Fludarabine (Green) and 5′-Dehydroadenosine (CHEBI: 1958) (Golden) showed nearly same RMSD value in his final steps of 100-ns simulation (Fig. 7a). The mobility of the protein (RMSF) values were not dissimilar except in some small regions (Fig. 7b). Protein compactness (Rg) and SASA decreased by the time (Fig. 7c and d).

The secondary structure contents were also similar between the approved drug–ligand complex and their corresponding proposed drug–ligand complex (Fig. 8). However, after ~ 20 ns a slight and stable increase in the 3-Helix was observed in L2R (Fig. 8a, b). After ~ 10-ns Coil structure was elevated in I4L (Fig. 8c, d).

Table 2 ChEMBL IDs of the approved drug Analogs that were detected using SwissSimilarity

Protein	Drugs (Commercial Name/ ChEMBL ID)
E8L (IMV surface membrane protein)	Brinzolamide CHEBI: 3176 CHEBI: 43411 Dorzolamide CHEBI: 4702 Methazolamide CHEBI: 6822
L2R (Thymidine Kinase)	Zidovudine CHEBI: 10110 CHEBI: 149753 CHEBI: 490877 CHEBI: 59847 CHEBI: 117980 CHEBI: 4728 CHEBI: 59846 CHEBI: 117936 CHEBI: 118100 CHEBI: 175144 CHEBI: 117931 CHEBI: 75473 CHEBI: 169114 CHEBI: 174448 CHEBI: 68294 CHEBI: 173933 CHEBI: 66159 CHEBI: 149757 CHEBI: 118107 CHEBI: 118121 CHEBI: 3578 CHEBI: 2453 CHEBI: 63581 CHEBI: 133856 CHEBI: 69770 CHEBI: 94793 CHEBI: 145220 CHEBI: 118075
I4L (Ribonucleotide reductase large subunit R1)	Gemcitabine CHEBI: 175901 Fludarabine CHEBI: 94701 CHEBI: 94359 CHEBI: 39740 CHEBI: 9978 CHEBI: 93913 CHEBI: 45327 CHEBI: 55419 CHEBI: 140569 CHEBI: 46515 CHEBI: 95180 CHEBI: 125640 CHEBI: 125449 CHEBI: 1014 CHEBI: 16335 CHEBI: 49751 CHEBI: 90031 CHEBI: 42452 CHEBI: 2310 CHEBI: 73141 CHEBI: 19688 CHEBI: 16750 CHEBI: 174609 CHEBI: 85997 CHEBI: 681569 CHEBI: 3927 CHEBI: 93920 CHEBI: 28498 CHEBI: 93817 CHEBI: 45448 CHEBI: 83079 CHEBI: 70972 CHEBI: 83080 CHEBI: 1958 CHEBI: 95153 CHEBI: 2312 CHEBI: 31858 CHEBI: 94463 CHEBI: 134989 CHEBI: 8612 CHEBI: 1196 CHEBI: 165834 CHEBI: 94738 CHEBI: 91901 CHEBI: 95211 CHEBI: 134606 CHEBI: 40167 CHEBI: 42575 CHEBI: 147281 CHEBI: 69426 CHEBI: 83081 CHEBI: 12060 CHEBI: 141077 CHEBI: 2038 CHEBI: 111177 CHEBI: 94323 CHEBI: 3202 CHEBI: 63580 CHEBI: 62005 CHEBI: 44081 CHEBI: 63612 CHEBI: 145115 CHEBI: 90239 CHEBI: 16299 CHEBI: 76278 CHEBI: 9976 CHEBI: 168049 CHEBI: 21891 CHEBI: 131374 CHEBI: 168240 CHEBI: 8098
Phospholipase-D-like protein	Tecovirimat CHEBI: 83194 CHEBI: 80011 CHEBI: 108514 CHEBI: 111390

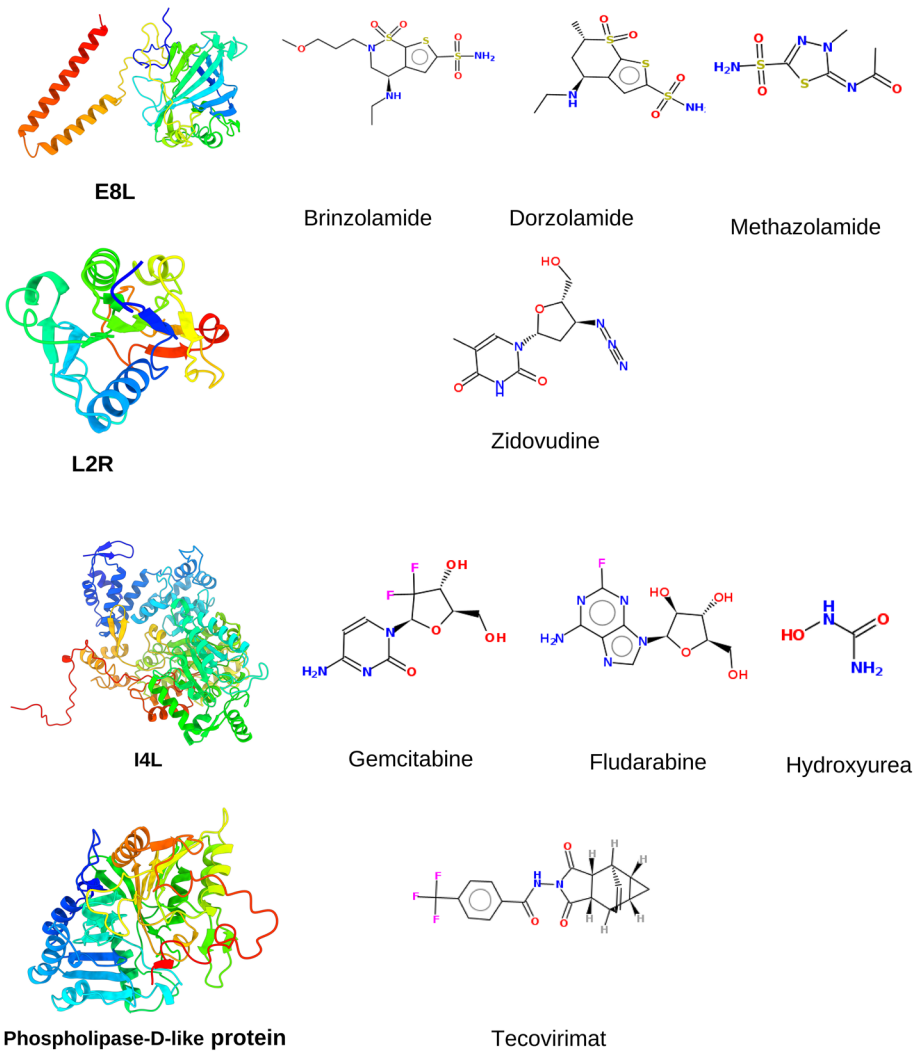

Fig. 2 Chemical structure of the selected approved drugs with the therapeutic targets. Chemical structures were generated using Molinspiration (https://www.molinspiration.com/)

Discussion

The monkeypox disease is difficult to control, especially in developing nations. Poor management and improper treatment might result in long-term illness with severe negative effects (6). For diagnosis, the virus can be detected with Polymerase Chain Reaction (PCR) tests. But treatment includes mainly Cidofovir and Tecovirimat. These drugs can reduce the duration of viral shedding with several side effects (30) (8). However, Tecovirimat is still on trial and depending solely on these drugs may exacerbate the situation with costs and drug-resistant variants. As a result, new drugs are required to control the spread of MPXV in both endemic and non-endemic countries.

Drug repurposing is a fast and viable solution to this problem. Bioinformatics-based screening can be used to repurpose existing medications at a preliminary level. In this study, we wanted to propose several approved drugs and other compounds that are similar to them with better mutagenicity and toxicity profiles. To do so, we explored the proteome of MPXV. Then selected E8L/IMV surface membrane protein and I4L/ ribonucleotide reductase large subunit R1 showed as druggable candidates. These proteins have strong sequence similarity and domains that can be targeted with Brinzolamide, Dorzolamide, Methazolamid, Gemcitabine, Hydroxyurea, and Fludarabine. For example, according to pfam (https://pfam.xfam.org/), E8L has a Eukaryotic-type carbonic anhydrase domain. Brinzolamide, Dorzolamide, or Methazolamide are carbonic anhydrase inhibitors that are used to treat glaucoma [30–32]. These carbonic anhydrase inhibitors also demonstrated antiviral properties against influenza virus and Severe acute respiratory syndrome coronavirus 2 (SARS-CoV-2) [33–35]. Therefore, Brinzolamide, Dorzolamide, or Methazolamide could potentially interfere

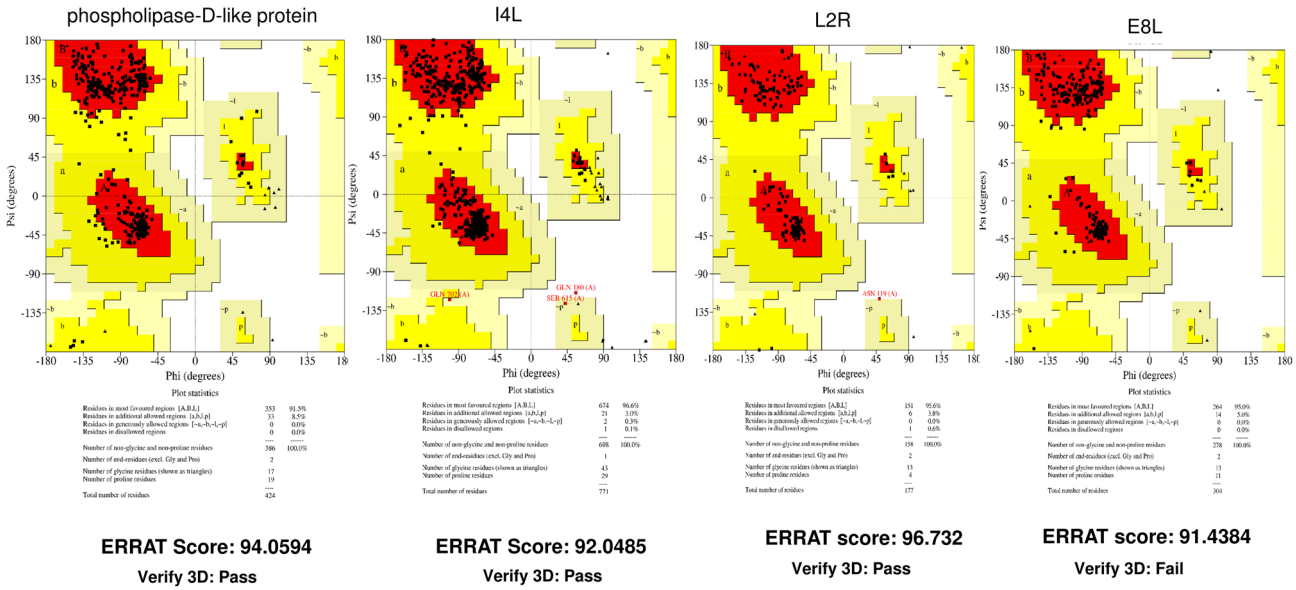

Fig. 3 Model validation of the receptors. Ramachandran plot, ERRAT scores, and Verify 3D represented the model quality. Phospholipase-D-Like protein, I4L, L2R and E8L had decent ERRAT scores and Ramachandran-favored regions percentages. Except E8L all of the structures passed Verify 3D parameter

in cell surface binding of IMV by inhibiting E8L Eukaryotic-type carbonic anhydrase domain. These drugs can be used as lead compounds to develop less toxic and mutagenic anti-MPXV agents. Moreover, I4L has Ribonucleotide reductase family (barrel domain), Ribonucleotide reductase (all-alpha domain) and ATP cone domain. Gemcitabine, Hydroxyurea, and Fludarabine-type nucleoside analogs could react with I4L and stop viral replication. Ribonucleotide Reductase is essential for generating DNA precursors and pathogenesis in poxviruses [36]. Gemcitabine, Hydroxyurea, and Fludarabine inhibit Ribonucleotide reductase in mammalian cells or interfere in DNA replication process. Gemcitabine and hydroxyurea have broad-spectrum antiviral or anti-Ribonucleotide reductase activity [37, 38]. Fludarabine can reduce the secretion of hepatitis B virus progeny DNA in HepG2-NTCPsec + cells [39]. Reasonably, these approved nucleoside analogs should reduce MPXV pathogenesis by decreasing MPXV DNA synthesis that are mediated by I4L. L2R protein has Thymidine kinase domain and Zidovudine, a dideoxynucleoside, can interact with this viral protein (https://go.drugbank.com/). Zidovudine has broad-spectrum thymidine kinase interference capability. This drug can inhibit thymidine incorporation in different mammalian, bacterial, and viral genomes [40–42]. Hence, if Zidovudine gets phosphorylated by L2R, it potentiates chain reaction termination during MPXV DNA replication.

To develop less hepatotoxic and non-mutagenic drugs, we searched for similar compounds using the 3D electroshape algorithm of SwissSimilarity. After collecting the compounds, molecular docking was conducted with their corresponding receptors. The molecular docking simulations revealed compounds that can interact with the receptors with satisfactory binding affinity scores (binding affinity score more than or equal to the approved drugs) (Table 3). Ki values more than 100 µM can be considered as potent inhibitors [43]. Except CHEBI 43411, CHEBI 6822 and Methazolamide, all of Table 3 compounds were potent inhibitors. The most potent inhibitor was Tecovirimat analog 2-((4-Methoxy-3-methyl-2-pyridylmethyl)sulfo)-5-trifluoromethyl-1H-benzimidazole (CHEBI:80011) with Ki value 0.412833. This benzimidazole can be further modified to develop better anti-MPXV drugs.

To execute the docking, the receptors were modeled using DeepMind's AlphaFold 2 (14). AlphaFold 2 is an artificial intelligence (AI)-based groundbreaking software that can model any protein from amino acid sequences with a very high level of accuracy. The models were refined for molecular docking. Compounds with equal or higher binding affinity scores were selected for pkCSM-based ADMET analysis. pkCSM demonstrated a harmala alkaloid (2S,4R)-4-(9H-Pyrido[3,4-b]indol-1-yl)-1,2,4-butanetriol (CHEBI: 173933) and 5′-Dehydroadenosine (CHEBI: 1958) showed decent intestinal absorption. After absorption, except this harmala alkaloid, all of these drugs will disseminate in unbound form (more than 70% of the absorbed drugs). During this circulation, they cannot cross

Table 3 Name of the approved drugs and their ChEMBL IDs. ChEMBL IDs of the analogs that exhibited higher binding scores with their corresponding receptors than the approved drugs

Ligand	Binding Affinity (kcal/mol) with L2R	Inhibition constant, μM (T = 298.15 K)
CHEBI: 68294	− 7.6	2.64835
CHEBI: 145220	− 7.2	5.20598
CHEBI: 175144	− 6.7	12.1175
CHEBI: 133856	− 6.6	14.3481
CHEBI: 173933	− 6.6	14.3481
CHEBI: 66159	− 6.5	16.9893
CHEBI: 149753	− 6.5	16.9893
CHEBI: 3578	− 6.2	28.2047
CHEBI: 75473	− 6.2	28.2047
CHEBI: 174448	− 6.2	28.2047
CHEBI: 490877	− 6.2	28.2047
CHEBI: 149757	− 6.1	33.3967
CHEBI: 10110	− 6	39.5445
CHEBI: 94793	− 6	39.5445
CHEBI: 117936	− 6	39.5445
CHEBI: 4728	− 5.9	46.8239
Zidovudine	− 5.9	46.8239
Ligand	Binding Affinity (kcal/mol) with I4L	Inhibition constant, μM (T = 298.15 K)
CHEBI: 95211	− 7.7	2.23663
CHEBI: 3202	− 7.3	4.39664
CHEBI: 168240	− 7.3	4.39664
CHEBI: 3927	− 7.2	5.20598
CHEBI: 95153	− 7.2	5.20598
CHEBI: 9976	− 7.1	6.16431
CHEBI: 55419	− 7	7.29905
CHEBI: 93920	− 7	7.29905
CHEBI: 45448	− 6.9	8.64268
CHEBI: 90031	− 6.9	8.64268
CHEBI: 94359	− 6.9	8.64268
CHEBI: 1196	− 6.8	10.2336
CHEBI: 16299	− 6.8	10.2336
CHEBI: 73141	− 6.8	10.2336
CHEBI: 85997	− 6.8	10.2336
CHEBI: 147281	− 6.8	10.2336
CHEBI: 2310	− 6.7	12.1175
CHEBI: 63580	− 6.7	12.1175
CHEBI: 94463	− 6.6	14.3481
CHEBI: 1014	− 6.5	16.9893
CHEBI: 31858	− 6.5	16.9893
CHEBI: 62005	− 6.5	16.9893
CHEBI: 83079	− 6.5	16.9893
CHEBI: 90239	− 6.5	16.9893
CHEBI: 168049	− 6.5	16.9893
CHEBI: 1958	− 6.4	20.1168
CHEBI: 8098	− 6.4	20.1168
CHEBI: 19688	− 6.4	20.1168
CHEBI: 42575	− 6.4	20.1168

Table 3 (continued)

Ligand	Binding Affinity (kcal/mol) with I4L	Inhibition constant, μM (T = 298.15 K)
CHEBI: 69426	− 6.4	20.1168
CHEBI: 83081	− 6.4	20.1168
CHEBI: 94738	− 6.4	20.1168
CHEBI: 165834	− 6.4	20.1168
Fludarabine	− 6.4	20.1168
Ligand	Binding Affinity (kcal/mol) with Phospholipase-D-like protein	Inhibition constant, μM (T = 298.15 K)
CHEBI: 80011	− 8.7	0.412833
Tecovirimat	− 8.6	0.488828
Ligand	Binding Affinity (kcal/mol) with E8L	Inhibition constant, μM (T = 298.15 K)
CHEBI__4702	− 6.4	20.1168
Dorzolamide	− 6.3	23.8199
CHEBI__3176	− 6	39.5445
Brinzolamide	− 5.6	77.7344
CHEBI__43411	− 5.4	108.988
CHEBI__6822	− 5.2	152.806
Methazolamide	− 4.9	253.68

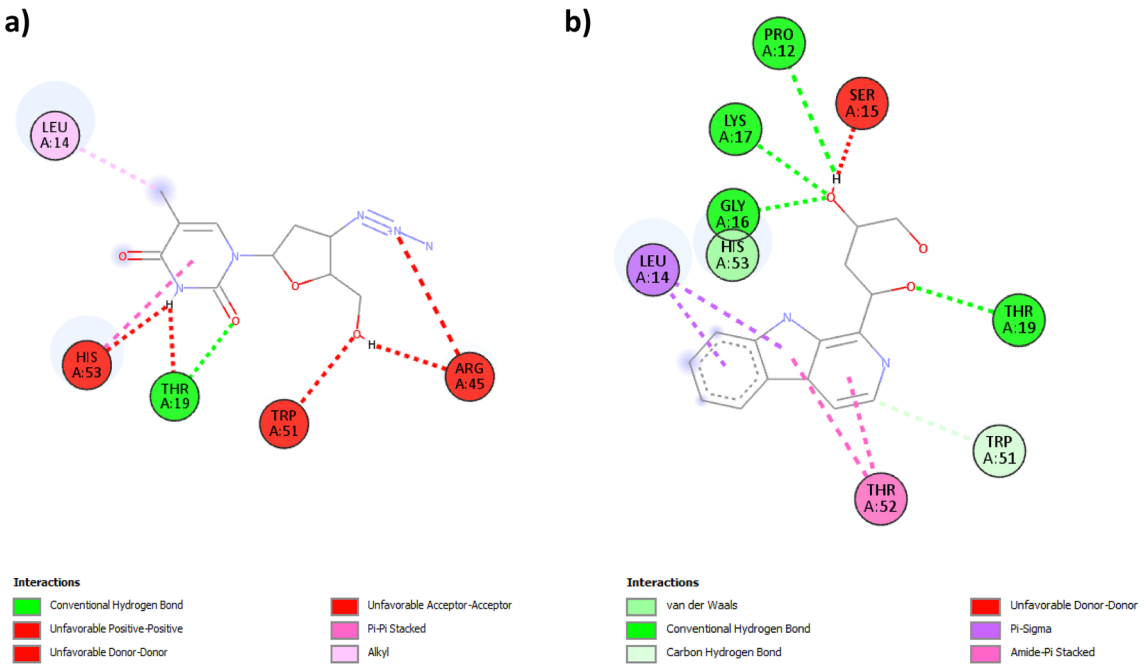

Fig. 4 L2R (Thymidine Kinase) interactions with **a** Zidovudine (binding affinity − 5.9 kcal/mol) and **b** (2S,4R)-4-(9H-Pyrido[3,4-b]indol-1-yl)-1,2,4-butanetriol (CHEBI: 173933) (binding affinity − 6.6 kcal/mol)

the blood–brain barrier or Central Nervous System (CNS). Plausibly, these drugs cannot interfere with the nervous system. None of these drugs can interact with cytochrome P450 (CYP) enzymes except (2S,4R)-4-(9H-Pyrido[3,4-b] indol-1-yl)-1,2,4-butanetriol (CHEBI: 173933). For this compound, drug–drug interactions and personalized medication might be more important. All of the drugs showed higher total clearance than 0.6 except Zidovudine

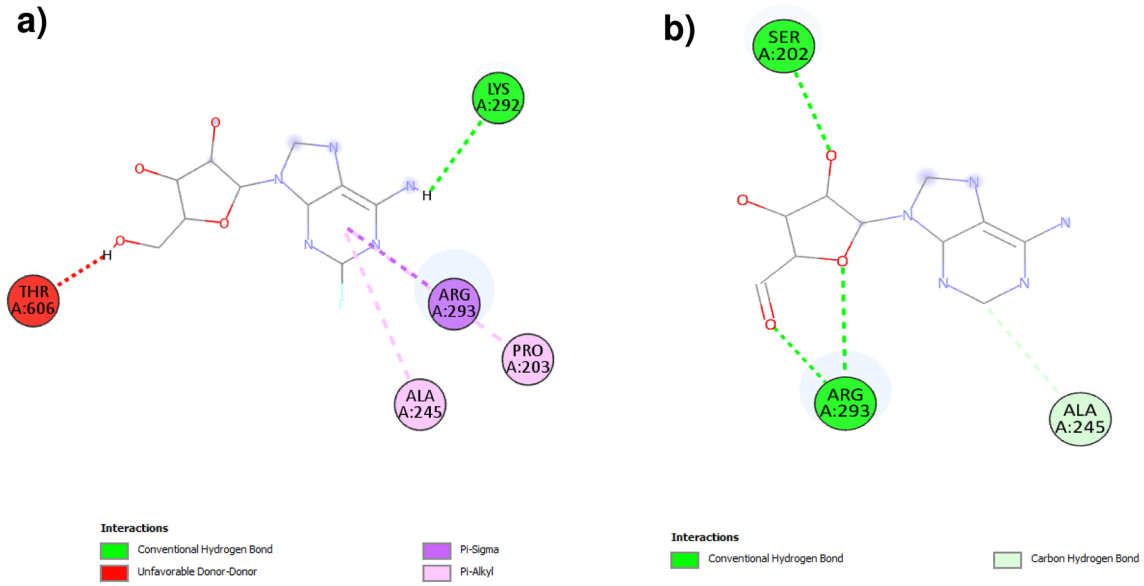

Fig. 5 I4L (Ribonucleotide reductase large subunit R1) interactions with **a** Fludarabine (binding affinity − 6.4 kcal/mol) and **b** 5′-Dehydroadenosine (CHEBI: 1958) (binding affinity − 6.4 kcal/mol)

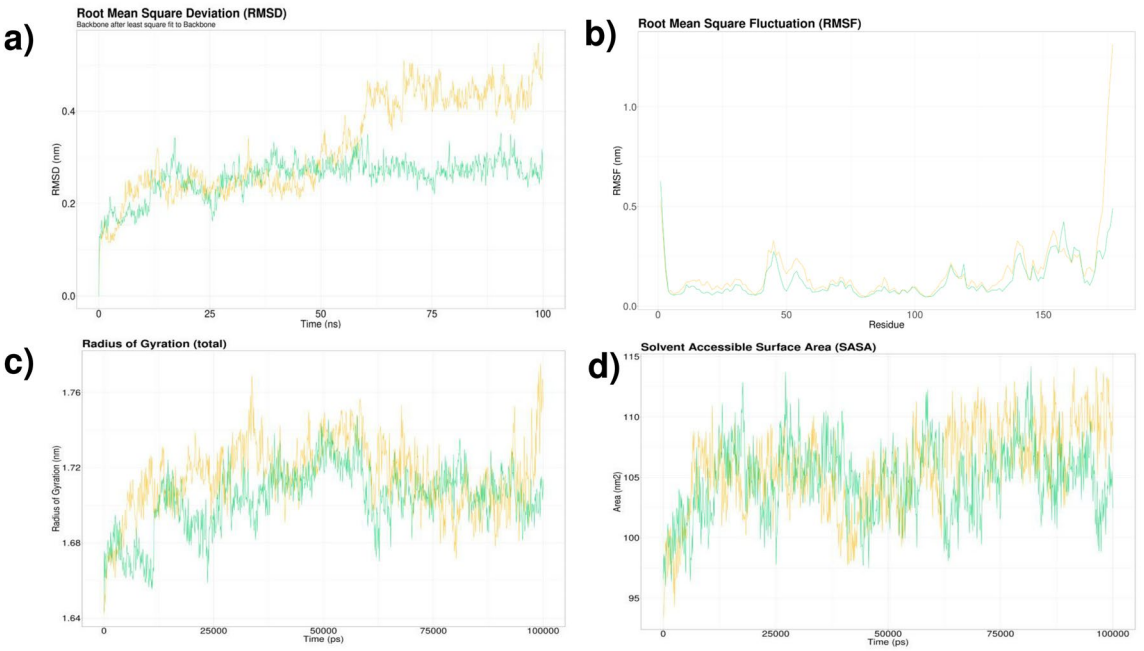

Fig. 6 Molecular dynamics simulation of L2R (Thymidine Kinase) with Zidovudine (Green) and (2S,4R)-4-(9H-Pyrido[3,4-b]indol-1-yl)-1,2,4-butanetriol (CHEBI: 173933) (Golden) where **a** 100-ns Root Mean Square Deviation (RMSD), **b** Root Mean Square Fluctuations (RMSF) of all residues, **c** Radius of Gyration (Rg) for 100,000 ps, and **d** Solvent-Accessible Surface Area (SASA) profile have been demonstrated. Here, RMSD represents the protein stability with the drugs inside the dynamic system. The RMSF graph depicts the mobility of the receptors with the drugs. Rg graph showing alteration of protein compactness during the simulation and SASA representing the change of solvent accessible surface in dynamic condition

(Table 4). Hence, to maintain a good bioavailability, these drugs should be administered in a higher amount than Zidovudine. Only Fludarabine tested positive for AMES, whereas all other medicines tested negative. pkCSM classified both the approved medications Zidovudine and Fludarabine as hepatotoxic. 5′-Dehydroadenosine and (2S,4R)-4-(9H- Pyrido[3,4-b]indol-1-yl)-1,2,4-butanetriol (CHEBI: 173933) had no hepatotoxic properties.

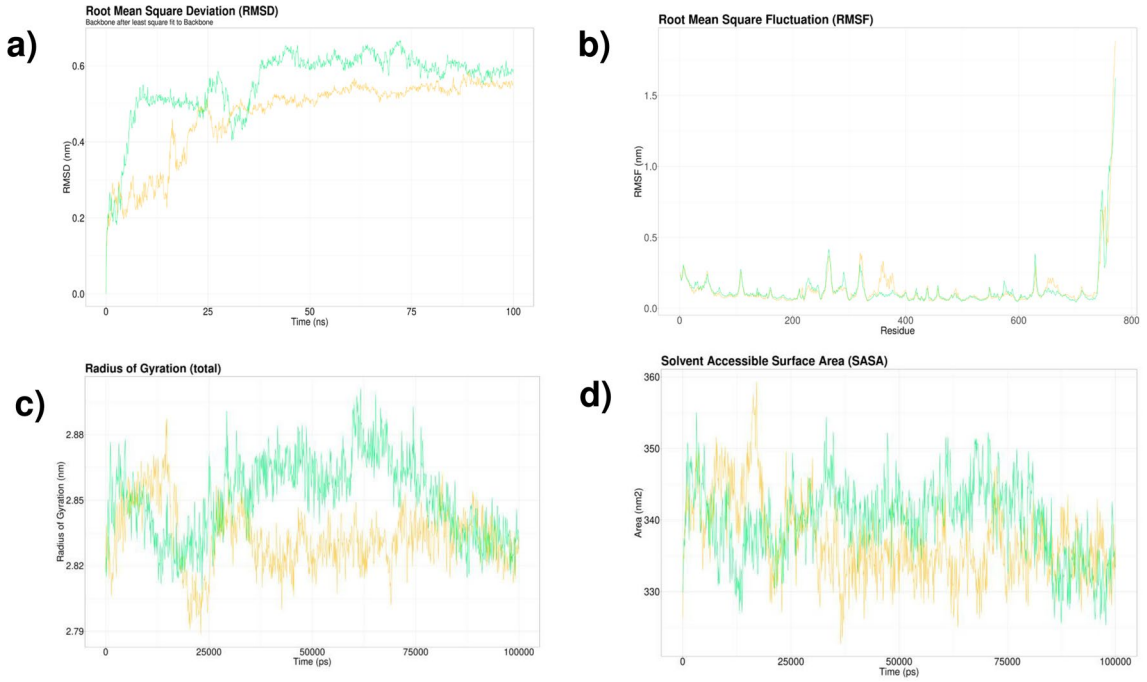

Fig. 7 Molecular dynamics simulation of I4L (Ribonucleotide reductase large subunit R1) with Fludarabine (Green) and 5′-Dehydroadenosine (CHEBI: 1958) (Golden) where **a** 100-ns Root Mean Square Deviation (RMSD), b) Root Mean Square Fluctuations (RMSF) of all residues, **c** Radius of Gyration (Rg) for 100,000 ps, and **d** Solvent-Accessible Surface Area (SASA) profile have been demonstrated. Here, RMSD represents the protein stability with the drugs inside the dynamic system. The RMSF graph depicts the mobility of the receptors with the drugs. Rg graph showing alteration of protein compactness during the simulation and SASA representing the change of solvent accessible surface in dynamic condition

Therefore, the similar compounds should be safe to use. Ligand–receptor Visualization revealed these analogs made less unfavorable bonds with the receptors and more conventional H bonds than their approved counterparts (Fig. 4 and 5). These bonds presented static interactions. To analyze them in dynamic conditions, MD simulation was conducted. MD simulation results suggested that these drugs can modulate the function of the viral proteins by manipulating the c-alpha backbones. These manipulations can change the mobility, compactness, and solvent accessible surface of the proteins. The secondary structure contents further support structural changes of the protein. GROMACS gmx do_dssp results of approved and proposed drugs were not significantly different (Fig. 8). L2R 3-Helix and I4L Coil structures demonstrated slight elevation during the simulation. Therefore, according to these results, inside the host cell, the I4L (Ribonucleotide reductase large subunit R1) and L2R (Thymidine Kinase) will not be able to process the DNA replication properly. Consequently, in the intermediate phase of the viral life cycle (~ 100-min' post-infection) the MPXV protein will not be able to generate new IMVs. A Smaller amount of viral double-stranded DNA will not trigger cGAS; IFI16 and DNA-PK in an abrupt way (5). Previous studies reported that (2S,4R)-4-(9H-Pyrido[3,4-b]indol-1-yl)-1,2,4-butanetriol (CHEBI: 173933)-type harmala alkaloids containing *Peganum harmala* L. seeds have antiviral activities in in vivo and in vitro models [44]. The approved candidate of this compound, Zidovudine or Azidothymidine, is a well-studied viral polymerase inhibitor (https://go.drugbank.com/drugs/DB00495). The other approved drug Fludarabine, fluorinated purine analog, inhibited Zika virus, Enterovirus A71, and Severe fever with thrombocytopenia syndrome virus (IC50 values below 1 μM) different cell lines such as Vero, U251 MG, BHK21, and HMC3 cells [45]. Similar candidate, 5′-Dehydroadenosine, is a non-fluorinated purine analog and has potential properties to act as an antiviral agent (7). In future studies, researchers and clinicians can use this drug discovery pipeline/methodology, approved and proposed drugs to treat MPXV infected in vitro and in vivo models.

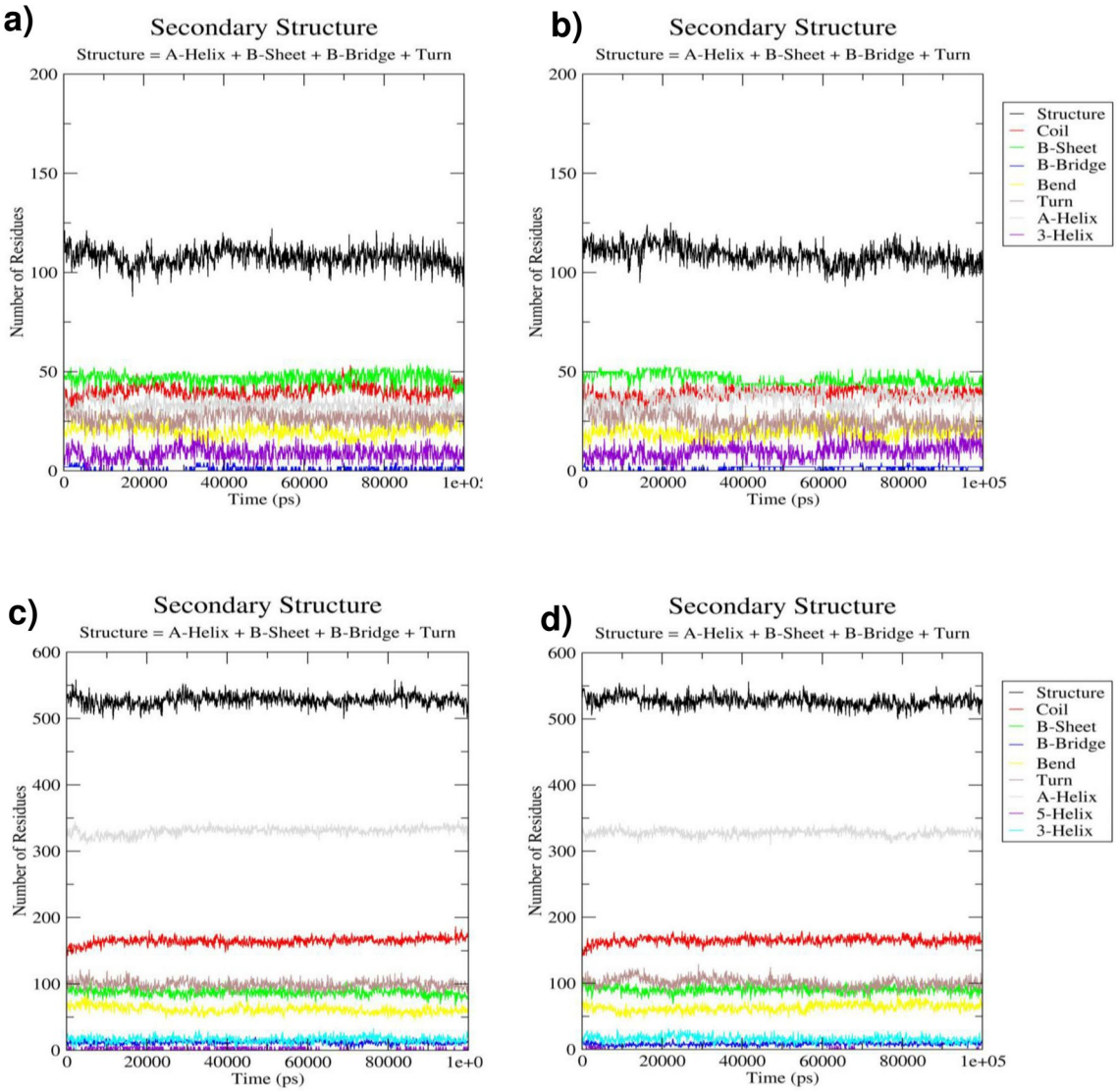

Fig. 8 Secondary structure contents of L2R (Thymidine Kinase) with **a** (2S,4R)-4-(9H-Pyrido[3,4-b]indol-1-yl)-1,2,4-butanetriol (CHEBI: 173933) and **b** Zidovudine. I4L (Ribonucleotide reductase large subunit R1) secondary structure contents with **c** 5′-Dehydroadenosine (CHEBI: 1958) and **d** Fludarabine

Conclusion

The MPVX infection can be targeted with Brinzolamide, Dorzolamide, Methazolamide, Zidovudine, Gemcitabine, Hydroxyurea, Fludarabine, and Tecovirimat. However, Zidovudine and Fludarabine analogs offer better druggable properties than others. Especially, our results suggest that Zidovudine, (2S,4R)-4-(9H-Pyrido[3,4-b]indol-1-yl)-1,2,4-butanetriol harmala alkaloid, Fludarabine, and 5′-Dehydroadenosine purine analog are potent antiviral agent and they can impede MPXV DNA synthesis by inhibiting or reacting with I4L (Ribonucleotide reductase large subunit R1) and L2R (Thymidine Kinase). This inhibition/reaction should prevent IMV and, eventually, EMV formation by depleting or masking A, T, G, and C. This in silico analysis encourages these drugs to be explored in in vivo and in vitro models for clinical applications.

Table 4 Absorption, Distribution, Metabolism, Excretion, and Toxicity properties of approved drugs and selected drugs

ADMET Properties	Zidovudine	(2S,4R)-4-(9H-Pyrido[3,4-b] indol-1-yl)-1,2,4-butanetriol [CHEBI: 173933]	Fludarabine	5′-Dehydroadenosine [CHEBI: 1958]
SMILES	CC1 = CN(C(=O) NC1 = O)C2CC(C(O2) CO)N = [N +] = [N-]	OCC(O)CC(O)C1 = NC = CC2 = C 1NC1 = C2C = C C = C1	C1 = NC2 = C(N = C(N = C2N1C3C(C(C(O3) CO)O)O)F)N	NC1 = C2N = CN([C@@H]3O[C@H] (C = O)[C@@H](O)[C@H]3O) C2 = NC = N1
MOL_WEIGHT	267.245	272.304	285.235	265.229
LOGP	− 0.19628	1.4928	− 1.8409	− 1.7734
#ROTATABLE_BONDS	3	4	2	2
#ACCEPTORS	6	4	9	9
#DONORS	2	4	4	3
SURFACE_AREA	106.629	115.066	111.012	106.213
Water solubility (log mol/L)	− 3.517	− 2.984	−2.101	− 1.516
Caco2 permeability (log Papp in 10–6 cm/s)	− 0.154	1.085	− 0.123	0.201
Intestinal absorption (human) (% Absorbed)	70.225	92.641	58.223	51.647
Skin Permeability (log Kp)	− 3.142	− 2.742	− 2.735	− 2.735
P-glycoprotein substrate	No	No	No	Yes
P-glycoprotein I inhibitor	No	No	No	No
P-glycoprotein II inhibitor	No	No	No	No
VDss (human) (log L/kg)	0.036	− 0.013	0.524	− 0.108
Fraction unbound (human) (Fu)	0.755	0.137	0.86	0.81
BBB permeability	− 1.166	− 1.001	− 1.33	− 1.217
CNS permeability	− 3.236	− 3.02	− 3.727	− 3.714
CYP2D6 substrate	No	No	No	No
CYP3A4 substrate	No	No	No	No
CYP1A2 inhibitor	No	Yes	No	No
CYP2C19 inhibitor	No	No	No	No
CYP2C9 inhibitor	No	No	No	No
CYP2D6 inhibitor	No	No	No	No
CYP3A4 inhibitor	No	No	No	No
Total Clearance (log ml/min/kg)	0.052	0.663	0.703	0.793
Renal OCT2 substrate	No	No	No	No
AMES toxicity	No	No	Yes	No
Max. tolerated dose (human)	0.656	0.748	0.823	0.702
hERG I inhibitor	No	No	No	No
hERG II inhibitor	No	Yes	No	No
Oral Rat Acute Toxicity (LD50) (mol/kg)	2.298	2.15	1.973	1.763
Oral Rat Chronic Toxicity (LOAEL) (log mg/kg_bw/day)	2.014	1.222	3.056	2.727
Hepatotoxicity	Yes	No	Yes	No
Skin Sensitization	No	No	No	No

Table 4 (continued)

ADMET Properties	Zidovudine	(2S,4R)-4-(9H-Pyrido[3,4-b] indol-1-yl)-1,2,4-butanetriol [CHEBI: 173933]	Fludarabine	5′-Dehydroadenosine [CHEBI: 1958]
T. Pyriformis toxicity (log ug/L)	0.118	0.333	0.285	0.285
Minnow toxicity (log mM)	3.145	0.131	4.504	3.083

References

1. Marennikova, S. S., & Moyer, R. W. (2005). Classification of poxviruses and brief characterization of the genus orthopoxvirus. *Orthopoxviruses Pathogenic for Humans*. https://doi.org/10.1007/0-387-25306-8_2
2. Jezek, Z., Grab, B., Szczeniowski, M. V., Paluku, K. M., & Mutombo, M. (1988). Human monkeypox: secondary attack rates. *Bulletin of the World Health Organization, 66*(4), 465.
3. Hutson, C. L., Olson, V. A., Carroll, D. D., Abel, J. A., Hughes, C. M., Braden, Z. H., … Regnery, R. L. (2009). A prairie dog animal model of systemic orthopoxvirus disease using West African and Congo Basin strains of monkeypox virus. *The Journal of general virology, 90*(Pt 2), 323–333. https://doi.org/10.1099/VIR.0.005108-0
4. McFadden, G. (2005). Poxvirus tropism. *Nature reviews. Microbiology, 3*(3), 201–213. https://doi.org/10.1038/NRMICRO1099
5. Lu, Y., & Zhang, L. (2020). DNA-sensing antiviral innate immunity in poxvirus infection. *Frontiers in Immunology*. https://doi.org/10.3389/FIMMU.2020.01637
6. MacNeil, A., Reynolds, M. G., Braden, Z., Carroll, D. S., Bostik, V., Karem, K., … Damon, I. K. (2009). Transmission of atypical varicella-zoster virus infections involving palm and sole manifestations in an area with monkeypox endemicity. *Clinical infectious diseases*. Doi:https://doi.org/10.1086/595552
7. Wnuk, S. F., Yuan, C. S., Borchardt, R. T., Balzarini, J., De Clercq, E., & Robins, M. J. (1997). Anticancer and antiviral effects and inactivation of S-Adenosyl-l-homocysteine hydrolase with 5′-carboxaldehydes and oximes synthesized from adenosine and sugar-modified analogues1. *Journal of Medicinal Chemistry, 40*(11), 1608–1618. https://doi.org/10.1021/JM960828P
8. LiverTox: Clinical and Research Information on Drug-Induced Liver Injury [Internet] - PubMed. (n.d.). Retrieved October 10, 2022, from https://pubmed.ncbi.nlm.nih.gov/31643176/
9. Yang, G., Pevear, D. C., Davies, M. H., Collett, M. S., Bailey, T., Rippen, S., … Jordan, R. (2005). An orally bioavailable antipoxvirus compound (ST-246) inhibits extracellular virus formation and protects mice from lethal orthopoxvirus challenge. *Journal of Virology, 79*(20), 13139. https://doi.org/10.1128/JVI.79.20.13139-13149.2005
10. Dotolo, S., Marabotti, A., Facchiano, A., & Tagliaferri, R. (2021). A review on drug repurposing applicable to COVID-19. *Briefings in Bioinformatics, 22*(2), 726–741. https://doi.org/10.1093/BIB/BBAA288
11. Xue, H., Li, J., Xie, H., & Wang, Y. (2018). Review of drug repositioning approaches and resources. *International Journal of Biological Sciences, 14*(10), 1232. https://doi.org/10.7150/IJBS.24612
12. Solanki, V., & Tiwari, V. (2018). Subtractive proteomics to identify novel drug targets and reverse vaccinology for the development of chimeric vaccine against Acinetobacter baumannii. *Scientific Reports, 2018*(81), 1–19. https://doi.org/10.1038/s41598-018-26689-7
13. Zoete, V., Daina, A., Bovigny, C., & Michielin, O. (2016). SwissSimilarity: A web tool for low to ultra high throughput ligand-based virtual screening. *Journal of Chemical Information and Modeling, 56*(8), 1399–1404. https://doi.org/10.1021/ACS.JCIM.6B00174
14. Jumper, J., Evans, R., Pritzel, A., Green, T., Figurnov, M., Ronneberger, O., … Hassabis, D. (2021). Highly accurate protein structure prediction with AlphaFold. *Nature 596*(7873), 583–589. https://doi.org/10.1038/s41586-021-03819-2
15. Mirdita, M., Schütze, K., Moriwaki, Y., Heo, L., Ovchinnikov, S., & Steinegger, M. (2022). ColabFold: making protein folding accessible to all. *Nature Methods, 19*(6), 679–682. https://doi.org/10.1038/s41592-022-01488-1
16. Heo, L., Park, H., & Seok, C. (2013). GalaxyRefine: Protein structure refinement driven by side-chain repacking. *Nucleic Acids Research, 41*(W1), W384–W388. https://doi.org/10.1093/NAR/GKT458
17. Pettersen, E. F., Goddard, T. D., Huang, C. C., Meng, E. C., Couch, G. S., Croll, T. I., … Ferrin, T. E. (2021). UCSF ChimeraX: Structure visualization for researchers, educators, and developers. *Protein Science, 30*(1), 70–82. https://doi.org/10.1002/PRO.3943
18. Colovos, C., & Yeates, T. O. (1993). Verification of protein structures: Patterns of nonbonded atomic interactions. *Protein Science, 2*(9), 1511–1519. https://doi.org/10.1002/PRO.5560020916
19. Lüthy, R., Bowie, J. U., & Eisenberg, D. (1992). Assessment of protein models with three-dimensional profiles. *Nature, 356*(6364), 83–85. https://doi.org/10.1038/356083A0
20. Laskowski, R. A., MacArthur, M. W., Moss, D. S., & Thornton, J. M. (1993). PROCHECK: A program to check the stereochemical quality of protein structures. *Journal of Applied Crystallography, 26*(2), 283–291. https://doi.org/10.1107/S0021889892009944
21. Morris, G. M., Ruth, H., Lindstrom, W., Sanner, M. F., Belew, R. K., Goodsell, D. S., & Olson, A. J. (2009). AutoDock4 and AutoDockTools4: Automated docking with selective receptor flexibility. *Journal of computational chemistry, 30*(16), 2785–2791. https://doi.org/10.1002/JCC.21256
22. Trott, O., & Olson, A. J. (2010). AutoDock Vina: Improving the speed and accuracy of docking with a new scoring function, efficient optimization and multithreading. *Journal of Computational Chemistry, 31*(2), 455. https://doi.org/10.1002/JCC.21334
23. Dallakyan, S., & Olson, A. J. (2015). Small-molecule library screening by docking with PyRx. *Methods in molecular biology (Clifton, N.J.), 1263*, 243–250. https://doi.org/10.1007/978-1-4939-2269-7_19
24. O'Boyle, N. M., Banck, M., James, C. A., Morley, C., Vandermeersch, T., & Hutchison, G. R. (2011). Open Babel: An open

chemical toolbox. *Journal of cheminformatics*. https://doi.org/10.1186/1758-2946-3-33
25. Ortiz, C.L.D., Completo, G.C., Nacario, R.C. et al. (2019). Potential Inhibitors of Galactofuranosyltransferase 2 (GlfT2): Molecular Docking, 3D-QSAR, and In Silico ADMETox Studies. *Scientific reports, 9*, 17096. https://doi.org/10.1038/s41598-019-52764-8
26. Lill, M. A., & Danielson, M. L. (2011). Computer-aided drug design platform using PyMOL. *Journal of Computer-Aided Molecular Design, 25*(1), 13–19. https://doi.org/10.1007/S10822-010-9395-8
27. Jo, S., Kim, T., Iyer, V. G., & Im, W. (2008). CHARMM-GUI: A web-based graphical user interface for CHARMM. *Journal of Computational Chemistry, 29*(11), 1859–1865. https://doi.org/10.1002/JCC.20945
28. Abraham, M. J., Murtola, T., Schulz, R., Páll, S., Smith, J. C., Hess, B., & Lindah, E. (2015). GROMACS: High performance molecular simulations through multi-level parallelism from laptops to supercomputers. *SoftwareX, 1–2*, 19–25. https://doi.org/10.1016/J.SOFTX.2015.06.001
29. Huang, J., Rauscher, S., Nawrocki, G., Ran, T., Feig, M., De Groot, B. L., … MacKerell, A. D. (2017). CHARMM36m: An improved force field for folded and intrinsically disordered proteins. *Nature Methods, 14*(1), 71. https://doi.org/10.1038/NMETH.4067
30. Armstrong, M. S., Morris, G. M., Finn, P. W., Sharma, R., Moretti, L., Cooper, R. I., & Richards, W. G. (2010). ElectroShape: Fast molecular similarity calculations incorporating shape, chirality and electrostatics. *Journal of Computer-Aided Molecular Design, 24*(9), 789–801. https://doi.org/10.1007/S10822-010-9374-0
31. Adler, H., Gould, S., Hine, P., Snell, L. B., Wong, W., Houlihan, C. F., … Hruby, D. E. (2022). Clinical features and management of human monkeypox: A retrospective observational study in the UK. *The Lancet Infectious Diseases, 22*(8), 1153–1162. https://doi.org/10.1016/S1473-3099(22)00228-6
32. Supuran, C. T. (2016). Drug interaction considerations in the therapeutic use of carbonic anhydrase inhibitors. *Expert Opinion on Drug Metabolism Toxicology, 12*(4), 423–431. https://doi.org/10.1517/17425255.2016.1154534
33. Josset, L., Textoris, J., Loriod, B., Ferraris, O., Moules, V., Lina, B., … Rosa-Calatrava, M. (2010). Gene expression signature-based screening identifies new broadly effective influenza a antivirals. *PLOS ONE*, *5*(10), e13169. https://doi.org/10.1371/JOURNAL.PONE.0013169
34. Pizzorno, A., Padey, B., Terrier, O., & Rosa-Calatrava, M. (2019). Drug repurposing approaches for the treatment of influenza viral infection: Reviving old drugs to fight against a long-lived enemy. *Frontiers in Immunology, 10*(3), 531. https://doi.org/10.3389/FIMMU.2019.00531/BIBTEX
35. Li, Z., Peng, M., Chen, P., Liu, C., Hu, A., Zhang, Y., … Chen, S. (2022). Imatinib and methazolamide ameliorate COVID-19-induced metabolic complications via elevating ACE2 enzymatic activity and inhibiting viral entry. *Cell Metabolism*, *34*(3), 424–440.e7. https://doi.org/10.1016/j.cmet.2022.01.008
36. Gammon, D. B., Gowrishankar, B., Duraffour, S., Andrei, G., Upton, C., & Evans, D. H. (2010). Vaccinia virus-encoded ribonucleotide reductase subunits are differentially required for replication and pathogenesis. *PLOS Pathogens, 6*(7), e1000984. https://doi.org/10.1371/JOURNAL.PPAT.1000984
37. Shin, H. J., Kim, C., & Cho, S. (2018). Gemcitabine and nucleos(t)ide synthesis inhibitors are broad-spectrum antiviral drugs that activate innate immunity. *Viruses*. https://doi.org/10.3390/V10040211
38. Bhave, S., Elford, H., & McVoy, M. A. (2013). Ribonucleotide reductase inhibitors hydroxyurea, didox, and trimidox inhibit human cytomegalovirus replication in vitro and synergize with ganciclovir. *Antiviral Research, 100*(1), 151–158. https://doi.org/10.1016/J.ANTIVIRAL.2013.07.016
39. Yang, J., König, A., Park, S., Jo, E., Sung, P. S., Yoon, S. K., … Windisch, M. P. (2021). A new high-content screening assay of the entire hepatitis B virus life cycle identifies novel antivirals. *JHEP Reports*, *3*(4), 100296. https://doi.org/10.1016/j.jhepr.2021.100296
40. Lewin, C. S., Allen, R. A., & Amyes, S. G. B. (1990). Mechanisms of zidovudine resistance in bacteria. *Journal of medical microbiology, 33*(4), 235–238. https://doi.org/10.1099/00222615-33-4-235
41. Guettari, N., Loubière, L., Brisson, E., & Klatzmann, D. (1997). Use of herpes simplex virus thymidine kinase to improve the antiviral activity of zidovudine. *Virology, 235*(2), 398–405. https://doi.org/10.1006/VIRO.1997.8706
42. Susan-Resiga, D., Bentley, A. T., Lynx, M. D., LaClair, D. D., & McKee, E. E. (2007). Zidovudine inhibits thymidine phosphorylation in the isolated perfused rat heart. *Antimicrobial Agents and Chemotherapy, 51*(4), 1142–1149. https://doi.org/10.1128/AAC.01227-06/ASSET/7C6C3C98-0F10-4C18-865F-9D75DD81E9E6/ASSETS/GRAPHIC/ZAC0040763970006.JPEG
43. Zheng, X., & Polli, J. (2010). Identification of inhibitor concentrations to efficiently screen and measure inhibition Ki values against solute carrier transporters. *European Journal of Pharmaceutical Sciences, 41*(1), 43–52. https://doi.org/10.1016/J.EJPS.2010.05.013
44. Moradi, M.-T., Karimi, A., Fotouhi, F., Kheiri, S., & Torabi, A. (2017). In vitro and in vivo effects of *Peganumharmala* L. seeds extract against influenza A virus. *Avicenna Journal of Phytomedicine, 7*(6), 519.
45. Gao, C., Wen, C., Li, Z., Lin, S., Gao, S., Ding, H., … Yu, Y. (2021). Fludarabine Inhibits Infection of Zika Virus, SFTS Phlebovirus, and Enterovirus A71. *Viruses*, https://doi.org/10.3390/V13050774